PHILOSOPHICAL TRANSACTIONS OF THE ROYAL SOCIETY A MATHEMATICAL, PHYSICAL & ENGINEERING SCIENCES

Infrared Laser Spectroscopy of Cations [and Discussion]

P. B. Davies, R. N. Dixon and R. J. Saykally

Phil. Trans. R. Soc. Lond. A 1988 **324**, 121-130
doi: 10.1098/rsta.1988.0005

Phil. Trans. R. Soc. Lond. A **324**, 121–130 (1988)
Printed in Great Britain

Infrared laser spectroscopy of cations

By P. B. Davies

Department of Physical Chemistry, University of Cambridge, Lensfield Road, Cambridge CB2 1EP, U.K.

The high-resolution infrared diode laser absorption spectra of several cations have been recorded and analysed. Most of the spectra were detected with an AC discharge and the velocity-modulation technique, with frequencies up to 60 kHz. In addition to ions, this method can also detect transient neutral species by recording at twice the modulation frequency (concentration modulation). As an example, spectra of an infrared electronic transition in H_2 are described briefly. The diatomic cationic species discussed are CO^+ ($X^2\Sigma^+$) and SH^+ ($X^3\Sigma^-$), which are compared with the isoelectronic neutral free radicals CN and PH respectively, also in their ground states. Polyatomic cations that have been studied include HCO^+ and H_3O^+. The bending mode of HCO^+ (2^1_0) shows a distinctive Q-branch with many resolved components at Doppler-limited resolution and also some hot-band lines. The HCO^+ spectrum can be combined with microwave measurements in the ground vibrational level to yield predictions for (2_1) rotational transitions for astrophysical searches. The most recent spectra of the ν_2 'umbrella' mode of H_3O^+, the $2^+ \leftarrow 1^-$ band, provide spectroscopic data on vibrational levels approximately 1000 cm^{-1} above the inversion potential maximum.

Introduction

Considerable progress has been made recently in our knowledge of the structure of simple ions. Pioneering work in high resolution spectroscopy by Woods and co-workers in the microwave region (Dixon & Woods 1975) and later by Oka (1980) in the infrared showed it was feasible to generate sufficient ion concentrations in discharges for absorption spectroscopy. These experiments were followed by many other studies of (mainly) cationic species as well as *ab initio* calculations of structural properties such as vibrational frequencies and internuclear distances (Botschwina 1986). Because the experimental techniques are not always wide ranging in their frequency coverage, accurate theoretical predictions, for the infrared region at least, are of considerable value. Alternative experimental data from, for example, matrix isolation or photoelectron spectroscopy are often unavailable. This contribution describes the infrared (IR) diode laser spectra of several free cations (including open-shell species) and compares their features with neutral isoelectronic analogues.

Experimental

The difficulty of distinguishing ions from neutrals in a discharge plasma has been overcome with the introduction of velocity modulation (Gudeman *et al.* 1983) and other techniques. However, if the chemical composition of the discharge is not too complicated and reliable predictions are available it is possible to extract IR spectra of ions without recourse to specially developed modulation techniques. Figure 1 is an example, a spectrum of HCl^+ recorded in

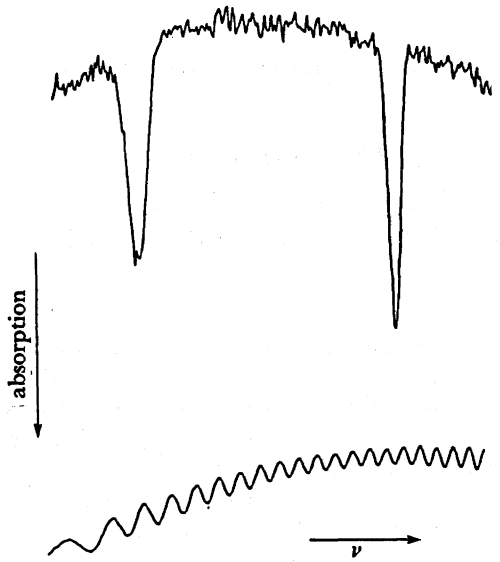

FIGURE 1. Infrared absorption spectrum of the $H^{35}Cl^+$ R(8.5) transition near 2720 cm^{-1} recorded with a 3 m DC discharge as ion source. The apparently unequal intensities of the two components arise from the slightly nonlinear frequency scale.

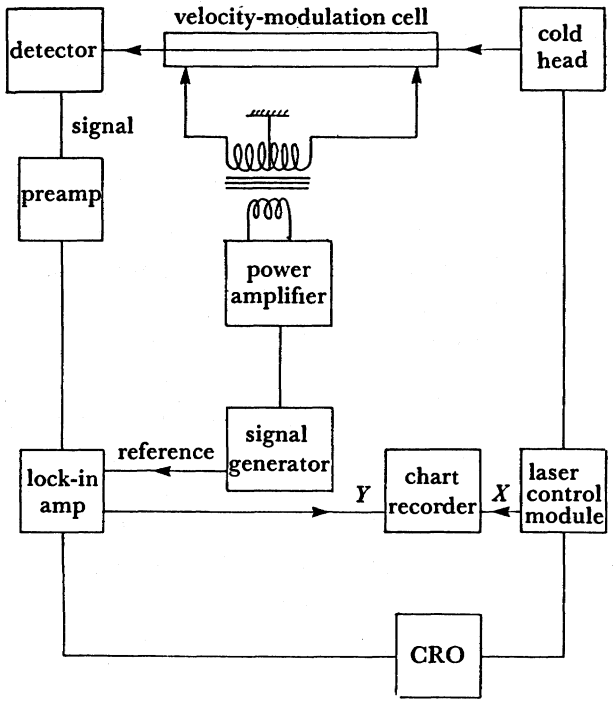

FIGURE 2. Experimental arrangement for velocity ($1f$) or concentration ($2f$) modulation detection of transient species generated in an AC discharge.

absorption by rapid-scan diode laser spectroscopy under computer control (Davies *et al.* 1983). This is a particularly favourable case, however, because very accurate electronic spectroscopy provides unambiguous assignments. This method of detection has now been superseded by velocity modulation. Measurement of noise at the detector with a spectrum analyser (Rothwell 1985) shows clearly that the frequency of the AC discharge used in velocity-modulation

experiments should be greater than 10 kHz. Figure 2 shows schematically the arrangement for velocity-modulation detection. The modulation wave form used is sinusoidal rather than square wave, and although this yields a lower 'duty cycle' for the discharge there is usually much less distortion of the waveform by the transformer.

An additional benefit of using an AC discharge is that tuning the phase sensitive detector to $2f$, twice the modulation frequency, a concentration modulation effect is observed and species with lifetimes shorter than $1/f$ (neutral or charged) can be detected with 'zeroth-order' absorption lineshapes. Figure 3 is a spectrum of molecular hydrogen observed in this way. The

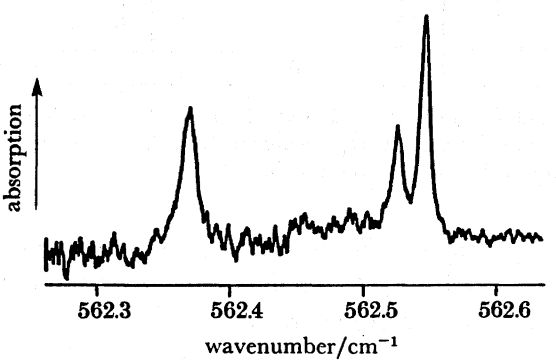

FIGURE 3. Absorption spectrum of excited H_2 generated in an AC discharge and detected by concentration modulation (at $2f$). The transition is the Q(2) component $\Delta v = 0$, $v = 2$ band of the a $\leftarrow$ c system. This is a transition in para-H_2 and shows fine structure but no hyperfine structure.

spectrum is part of the infrared a–c electronic transition in H_2 which can be observed in absorption or emission in a hydrogen plasma (Davies *et al.* 1987). Finally, the potential of using an AC discharge to investigate dynamical in addition to purely spectroscopic behaviour has yet to be fully realized. Preliminary work on infrared transitions in Rydberg states of the O atom has shown that the decay of transient species can be followed in real time as the discharge switches on and off (P. R. Brown and P. A. Hamilton, unpublished results).

RESULTS

The four diatomic molecules described here are all free radicals and have quenched orbital angular momentum. The structure of their rotational and fine-structure levels can be classified as Hund's case (*b*). One pair have $^2\Sigma$ ground state and the other $^3\Sigma$. Figure 4 is a schematic energy level diagram for both cases. The infrared spectra consist of P-branches and R-branches only and for each rotational component $\Delta J = \Delta N$ transitions are usually the most intense except near the band origin.

CN, CO^+ ($X\ ^2\Sigma^+$)

For the R- and P-branches of the fundamental band the doubling of each line in the spectrum ($\Delta J = \Delta N = \pm 1$) is determined by the interaction of the unpaired electron with the rotation of the molecule, $\gamma_v \boldsymbol{N}\cdot\boldsymbol{S}$, and is given by

$$N(\gamma_1-\gamma_0)+\tfrac{1}{2}(3\gamma_1-\gamma_0), \quad \text{R-branch},$$
$$N(\gamma_1-\gamma_0)-\tfrac{1}{2}(\gamma_1+\gamma_0), \quad \text{P-branch},$$

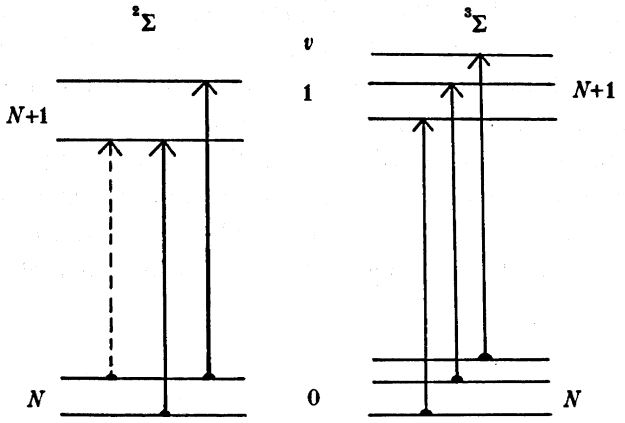

FIGURE 4. Fine structure of diatomic free radicals in $^2\Sigma$ and $^3\Sigma$ states. The transitions shown by solid vertical lines are $\Delta J = \Delta N$ components and the broken line represents the $\Delta J \neq \Delta N$ component (in the $^2\Sigma$ case). The energy levels and transitions are appropriate for the R-branch.

where γ is the spin-rotation parameter. For $2 < N < 10$ these expressions are approximately independent of rotation and the splitting of each line is $\bar{\gamma}$($\bar{\gamma} \approx 0.01$ and 0.007 cm^{-1} for CO^+ and CN respectively). For the $\Delta J = 0$ satellite we have

$$(\gamma_0 N + \tfrac{1}{2}\gamma_0) \text{ lower}, \quad \text{R-branch},$$
$$(\gamma_0 N + \tfrac{1}{2}\gamma_0) \text{ higher}, \quad \text{P-branch},$$

where 'lower' and 'higher' refers to the position relative to the main $\Delta J = \Delta N$ pair. The satellite line gains in intensity at lower N and for R(1) and P(2) is sufficiently close to the $\Delta J = \Delta N$ pair that triplets rather than doublets appear. At R(0) and P(1) only one $\Delta J = \Delta N$ transition is possible but for these rotational components doublet fine structure is still observed because of the satellite line.

Figure 5 shows the R(0) line of CN and, inset, the predicted relative intensities in the fine

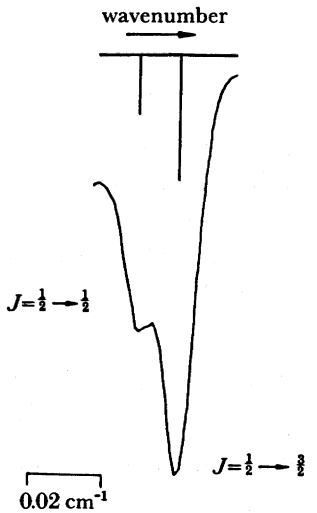

FIGURE 5. Diode laser spectrum of the R(0) transition of the fundamental band of CN($X^3\Sigma^+$) with resolved fine-structure components. Calculated positions and their relative intensity are shown at the top of the figure. The spectrum was recorded by using rapid-scan spectroscopy under computer control (Davies *et al.* 1983).

structure (Davies & Hamilton 1982). Many other transitions were observed with doublet splittings given by the formula above. Figure 6 shows the R(1) component of CO^+ with the predicted triplet fine structure (Davies & Rothwell 1985). (The different lineshapes for CN and CO^+ reflect the different modulation techniques used.)

PH, SH^+ ($X\ ^3\Sigma^-$)

As shown in figure 4, the main fine structure expected in the fundamental band of these molecules is a triplet splitting. Figure 7 shows the P(7) component of PH. The radical was formed in a DC discharge of molecular hydrogen over small amounts of elemental phosphorus (Anacona *et al.* 1984). The size of the spin–spin parameter, λ, in the ground state of PH results

FIGURE 6. The R(1) component of the fundamental band of CO^+ ($X^2\Sigma^+$) recorded with velocity-modulation detection. Peaks b and c are the $\Delta J = +1$ components, peak a is the single $\Delta J = 0$ transition. The calculated relative intensities are a:b:c, 1:5:9.

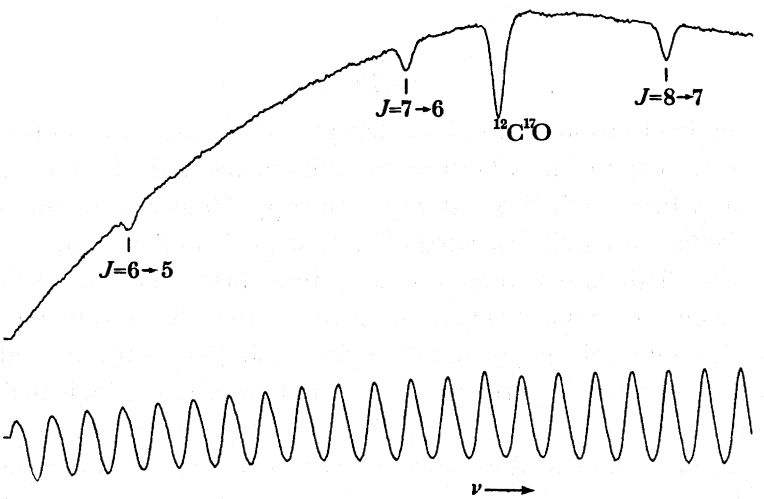

FIGURE 7. Diode laser absorption spectrum of the P(7) transition in PH ($X^3\Sigma^-$) showing the three fine-structure components. The calibration line from $^{12}C^{17}O$ in natural abundance is provided by CO at low pressure in a 15 cm long reference cell.

in a triplet fine structure approximately the same in magnitude as the wavenumber coverage of a single mode of this particular diode. In SH^+, λ is larger (SH^+, $\lambda \approx 5.78\ cm^{-1}$; PH, $\lambda \approx 2.21\ cm^{-1}$) but triplet structure is still visible, and figure 8 shows the fine structure of one of many components recorded in the fundamental band of SH^+ (Brown *et al.* 1986). Also shown in figure 8 is an additional line due to another cationic species. Possible candidates are electronically excited SH^+ (i.e. $^1\Delta$ or $^1\Sigma$), H_2S^+ or H_3S^+. On the right of the spectrum is another first-derivative line due to an ion but this peak is of opposite phase and arises from SH^- ($X\ ^1\Sigma^+$).

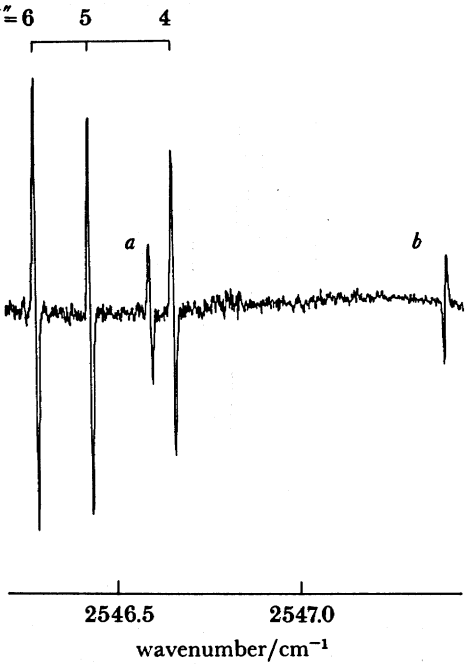

FIGURE 8. Velocity-modulation spectrum around the R(5) region of SH^+ ($X^3\Sigma^-$) showing the expected triplet fine structure. Line *a* arises from another cationic species and line *b* is a vibration–rotation transition in SH^- ($X^1\Sigma^+$).

HCO^+

This linear cation, isoelectronic with HCN, has played a central role in the development of high-resolution spectroscopy of ions both in the microwave and infrared regions. All three fundaments have now been studied by laser spectroscopy. However, for the stretching modes individual rotational lines are well separated ($\bar{B} \approx 1.48\ cm^{-1}$) and only one transition at a time can be recorded with diode lasers (there are no Q-branches). The Q-branch of the bending mode, however, presents a compact but well-resolved feature that can be recorded with good signal to noise ratios with velocity modulation detection (figure 9). In addition to intense fundamental lines, additional features from hot-band transitions, indicated by *, are also present in figure 9. As well as the purely spectroscopic study of this ion (Davies & Rothwell 1984), the IR laser results can be used to provide predictions for rotational transitions in excited vibrational states for astrophysical purposes. By combining three microwave measurements in the ground state of the ion with six diode laser measurements it is possible to arrive at predictions for two rotational transitions in the 2_1 level. The relevant measurements are given in table 1.

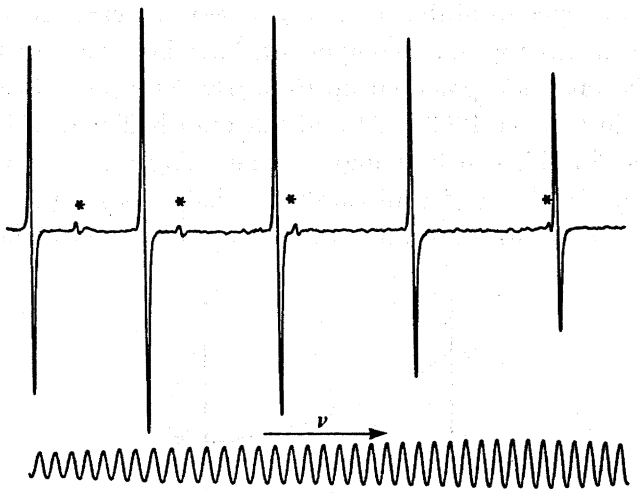

FIGURE 9. Part of the Q-branch of the ν_2 fundamental of HCO^+ near 830 cm^{-1}.

At the time these IR measurements were made, the most accurate calibration procedure available was to use standard gas-calibration lines and germanium etalons as interpolation devices. This limited the accuracy to ± 0.001 cm^{-1}, which was insufficient to yield an unambiguous prediction for radioastronomical purposes (L. Ziurys, personal communication). However, remeasurement of the IR transitions with a confocal Fabry–Perot etalon should improve the accuracy of the IR laser measurements by up to a factor of ten.

H_3O^+

This cation is probably the best example where experiment and theory complement each other. The ν_2 umbrella mode of the molecule has been of particular interest to spectroscopists

TABLE 1. PREDICTED ROTATIONAL TRANSITION FREQUENCIES IN VIBRATIONALLY EXCITED HCO^+

Diode laser results for the 2^1_0 band

line	measured wavenumber[a]	number of measurements	1 σ	calculated wavenumber[b]	difference
P(4)	816.3224	3	0.0003	816.3222	+0.0002
P(3)	819.3015	7	0.0007	819.3006	+0.0009
Q(2)	828.2694	6	0.0010	828.2685	+0.0006
Q(3)	828.3066	6	0.0011	828.3056	+0.0010
R(1)	834.1757	5	0.0018	834.1761	−0.0004
R(2)	837.1466	7	0.0018	837.1463	+0.0003

Rotational transitions from ground-state microwave spectroscopy[c]

$J''+1 \leftarrow J''$		wavenumber/cm^{-1}
4	3	11.899375 (2)
3	2	8.9247615 (3)
2	1	5.949952 (2)

Predicted line positions in the 2^1 level

$3^+ \leftrightarrow 2^-$	8.9620 ± 0.001 cm^{-1}
$3^- \leftrightarrow 2^+$	8.9203 ± 0.001 cm^{-1}

[a] P. A. Martin (unpublished results).
[b] Davies & Rothwell (1984).
[c] Sastry *et al.* (1981).

and theoreticians. IR laser spectra of this mode (ν_2, $1^- \leftarrow 0^+$) were first recorded by Haese & Oka (1984) and since then many other components have been recorded providing a rather complete picture of the inversion potential up to nearly 2000 cm^{-1} (Sears *et al.* 1985). The barrier to planarity is just under 1000 cm^{-1} and less than half that of isoelectronic NH_3. A qualitative explanation for this can be found by examining the appropriate Walsh orbital diagram for the...$(2a_1)^2$ $(1e)^4$ $(3a_1)^2$ configuration, which is shown in figure 10. The $2a_1$–$2a_1'$ and degenerate 1e–1e′ orbitals are little affected by the loss of planarity and are gently

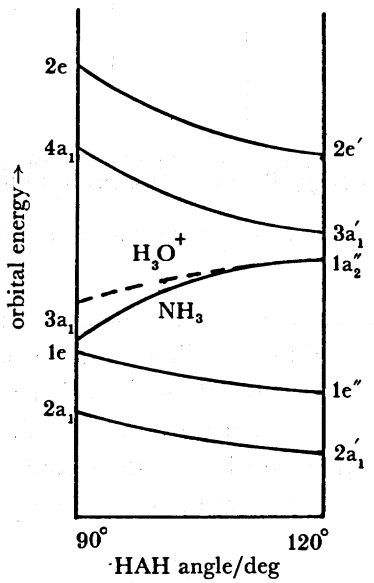

FIGURE 10. Walsh molecular orbitals for AH_3 species.

repulsive as the molecule becomes non-planar. The $3a_1$–$1a_2''$ orbital, comprising an out-of-plane 2p orbital on the heavy atom and H 1s orbitals, is strongly bonding in a non-planar configuration. In H_3O^+ (in comparison with NH_3), the positive charge located on the O-atom contracts the 2p orbital and raises the energy of the $3a_1$–$1a_2''$ molecular orbital relative to its position in NH_3, as indicated in figure 10. Numerous quantitative calculations of the inversion potential have been made (Botschwina 1986) and provide vibrational frequencies and bond lengths essential for experimental spectroscopic searches and interpretation of the very extensive infrared spectrum of H_3O^+.

The results reported here were obtained in collaboration with many colleagues whose names appear in the referenced work. I express my warmest thanks to them for their participation in this work and for many stimulating discussions.

REFERENCES

Anacona, J. R., Davies, P. B. & Hamilton, P. A. 1984 *Chem. Phys. Lett.* **104**, 269–271.
Botschwina, P. 1986 *J. chem. Phys.* **84**, 6523–6524.
Brown, P. R., Davies, P. B. & Johnson, S. A. 1986 *Chem. Phys. Lett.* **132**, 582–584.
Davies, P. B. & Hamilton, P. A. 1982 *J. chem. Phys.* **76**, 2127–2128.

Davies, P. B., Hamilton, P. A., Lewis-Bevan, W. & Okumura, M. 1983 *J. Phys. E.* **16**, 289–294.
Davies, P. B. & Rothwell, W. J. 1984 *J. chem. Phys.* **81**, 5239–5240.
Davies, P. B. & Rothwell, W. J. 1985 *J. chem. Phys.* **83**, 5450–5452.
Davies, P. B., Guest, M. A. & Johnson, S. A. 1987 (In preparation).
Dixon, T. A. & Woods, R. C. 1975 *Phys. Rev. Lett.* **34**, 61–63.
Gudeman, C. S., Begemann, M. H., Pfaff, J. & Saykally, R. J. 1983 *Phys. Rev. Lett.* **50**, 727–731.
Haese, N. N. & Oka, T. 1984 *J. chem. Phys.* **80**, 572–573.
Oka, T. 1980 *Phys. Rev. Lett.* **45**, 531–534.
Rothwell, W. J. 1985 Ph.D. thesis, University of Cambridge.
Sastry, K. V. L. N., Herbst, E. & DeLucia, F. C. 1981 *J. chem. Phys.* **75**, 4169–4170.
Sears, T. J., Bunker, P. R., Davies, P. B., Johnson, S. A. & Spirko, V. 1985 *J. chem. Phys.* **83**, 2676–2685.

Discussion

R. N. Dixon, F.R.S. (*School of Chemistry, University of Bristol, U.K.*). Dr Davies has commented that the inversion barrier of H_3O^+ is less than half of the isoelectronic NH_3 molecule; and it has been proposed that similar comparisons may be made between pairs of ions and molecules of the general type $AH_2^{(+)}$. It has been suggested that this might be attributed to a variation in the angular dependence of the orbital energy for the highest occupied orbital.

However, it must be pointed out that the excitation energy for the $\tilde{A}^2A_1$–$\tilde{X}^2B_1$ transition of H_2O^+ is little different from that of NH_2; this would not be the case on the above postulate. I suggest that this is a simple electrostatic effect. The substitution of N by O^+ will tend to polarize the whole electronic structure by withdrawing electrons from around the H nuclei. These nuclei are therefore less shielded, so that H–H nuclear repulsion will tend to open up the HAH angles, decreasing the inversion barriers between all such isoelectronic pairs in equivalent electronic states. On this basis it seems probable that CH_3^- would be more strongly pyramidal than NH_3, with a larger barrier to inversion in its ground electronic state: these shifts should be smaller than between H_3O^+ and NH_3 because of an increasing AH bond length along the series H_3O^+, NH_3 and CH_3^-.

P. B. Davies. The relative contributions of orbital energy and electrostatic effects in determining the inversion barrier in $H_3A^{(+)}$ molecules cannot be readily separated. The energy of the highest-occupied (Walsh) orbital, $3a_1 - 1a_2''$, is strongly angular dependent and is likely to play a major part in determining geometry. The contraction of the heavy atom p-orbital contributing to this molecular orbital as N (in NH_3) is replaced by O^+ (in H_3O^+) makes it less bonding in the non-planar configuration. This effect is in the same direction as the electrostatic effect suggested by Professor Dixon.

R. J. Saykally (*University of California, Berkeley, U.S.A.*). Regarding Dr Davies's analysis of the $\nu_2 = 2$ levels of H_3O^+, has he included Coriolis mixing in his hamiltonian? We have recently completed an analysis of the ν_4 band, and find that the upper ν_4 levels are strongly Coriolis mixed with nearly ν_2 states, resulting in large changes in the rotational constants.

P. B. Davies. In our analysis of the $\nu_2 2^+ \leftarrow 1^-$ band, four of the lines measured were poorly fitted and excluded from the final least squares fit. We gave the most likely explanation as Coriolis interaction with the $\nu_4 = 1$, recognizing that this effect could only be fully accounted for when ν_4 band data were available. It is also worth noting that the signs of the centrifugal

distortion parameters for the 2^+ level may also affect this. Nevertheless the published parameters are a reasonable representation of the 2^+ level for the lines we have measured (r.m.s. error = 0.006 cm^{-1}).

Reference

Davies, P. B., Johnson, S. A., Hamilton, P. A. & Sears, T. J. 1986 *Chem. Phys.* **108**, 335.

R. J. Saykally. Dr Davies described his measurements on the bending hot band of HCO^+, designed to provide precise constants for rotational transitions in the lowest excited bending mode to aid radio astronomy searches. My group has recently completed measurements of several pure rotational transitions in the $v_2 = 1$ state of HCO^+ by tunable far-infrared laser spectroscopy. We can now predict all astrophysically important transitions in the first excited bending state with about 100 kHz uncertainties, clearly sufficient precision to identify radio-astronomical spectra in this state.

Reference

Blake, G., Laughlin, K., Cohen, R., Busarow, K. & Saykally, R. J. 1987 *Astrophys. J.* (In the press.)

P. B. Davies. The recent introduction of confocal etalons for calibrating diode laser spectra will lead to a considerable improvement in measurement accuracy over methods using germanium etalons (accuracy of order 30 MHz). With a confocal Fabry–Perot etalon it has been shown that diode laser frequency stability of 100 kHz can be achieved. However, linewidths in the far-infrared region are lower than in the mid-infrared, which intrinsically contributes to better measurement precision.

Reference

Reich, M., Schieder, R., Clar, H. J. & Winnewisser, G. 1986 *Appl. Opt.* **25**, 130.

PHILOSOPHICAL TRANSACTIONS OF THE ROYAL SOCIETY A MATHEMATICAL, PHYSICAL & ENGINEERING SCIENCES